Comparison of methods of estimating mean synoptic current structure in "stream coordinates" reference frames with an example from the Antarctic Circumpolar Current

Christopher S. Meinen*, Douglas S. Luther

University of Hawaii at Manoa, Honolulu, HI, USA

Abstract

Stream coordinates techniques, that is, methods of deriving the mean "synoptic" structures of narrow meandering ocean currents from Eulerian measurements, have been in use for nearly two decades and have resulted in improvements in our understanding of the dynamics and transports of such currents. A 2-year experiment in the Sub-Antarctic Front (SAF) southwest of Tasmania, involving overlapping arrays of inverted echo sounders and horizontal electric field recorders, has provided an opportunity to test various stream coordinates methods. The methods differ significantly in how well, or even if, they can reveal divergence or convergence of the meandering current, and whether they accurately reproduce the current's horizontal structure and transport. Cross-stream distance was determined either via a frozen-field assumption or as the distance to an optimally interpolated (OI) origin contour; downstream direction was determined either as the local direction which maximized the vertical shear of horizontal velocity or as the tangent line to the OI mapped core contour. All combinations of these distance and direction definitions were tested. The use of a frozen field assumption in determining cross-stream distance yields overly smooth along-stream velocity cross-sections and overestimated transports. The vertical shear definition of downstream direction results in a false rotation of cross-stream flows into along-stream flows near the flanks of the current. The preferred methods define the horizontal location of the front with 2-D arrays of instruments (e.g., inverted echo sounders or moored current meters). Methods employing the assumptions of a meandering "frozen-field" baroclinic structure or the use of the local vertical shear of the horizontal velocity to determine the downstream direction should be avoided, if possible, particularly in the SAF.

1. Introduction

Temporal averaging of a strong meandering ocean current in Eulerian coordinates leads to

---

*Corresponding author. Current address: Cooperative Institute for Marine and Atmospheric Studies, University of Miami, 4301 Rickenbacker Causeway, Miami, FL, 33149, USA.

E-mail address: christopher.meinen@noaa.gov (C.S. Meinen).

well-known interpretational problems, such as underestimation of cross-stream gradients. Furthermore, the time-means of many quantities which are important to understanding the dynamics of oceanic currents are poorly estimated in Eulerian coordinates. Using individual snapshot sections to estimate the synoptic structure of a current has the well-known problem that any section could be "contaminated" by eddies and other smaller scale processes. For these and other

reasons a better method of estimating the mean synoptic structure of a current is needed. The method generally used to obtain the synoptic structure of a current is the "stream coordinates" approach. Stream coordinates techniques have been applied to strong current systems around the world, such as the Gulf Stream (Halkin and Rossby, 1985; Hall, 1986; Hogg, 1992; Johns et al., 1995; Bower and Hogg, 1996), the North Atlantic Current (Meinen, 2001), the Kuroshio extension (Hall, 1989), and the Subantarctic Front (Phillips and Rintoul, 2002).

The details of the application of stream co-ordinates in these studies differ. There are essentially three steps to conversion of Eulerian velocity measurements into stream coordinates: first, a definition of the center of the front/current must be chosen (i.e. the origin of a new Cartesian coordinate system fixed to the current); second, the location of each measurement site relative to that time-dependent center must be determined; and third, the velocities must be rotated from north-ward and eastward into "along-stream" and "cross-stream" components. For scalar quantities, such as temperature measurements, only the first two steps are relevant. The aforementioned studies have taken different approaches to each of the conversion steps, and, as will be shown, these differences can be important.

A large field experiment in 1995–1997, the Sub-Antarctic Flux and Dynamics Experiment (SAFDE), has provided the measurements needed for the analyses reported here. Among the instru-ments deployed in SAFDE was a large array of inverted echo sounders (IESs) and a long line of horizontal electric field recorders (HEFRs) (Luther et al., 1997). The SAFDE's large number of instruments provide an ideal data set for comparing different methods of obtaining stream coordinates representations of a current. The purpose of this paper is to demonstrate the strengths and weaknesses of the various methods and to present the best method for the Sub-antarctic Front (SAF). The SAF is the northern of the two strongest branches of the Antarctic Circumpolar Current (ACC) and it separates the relatively warm waters of the Subantarctic Zone from the relatively cold waters of the Polar Frontal Zone (Whitworth, 1983; see also Figs. 4.6.2 and 4.6.3 in Rintoul et al., 2001). Future papers will discuss the dynamical results obtained as part of this study.

2. Data

In the SAFDE, a large array of IESs and HEFRs, along with a few current meter moorings, were deployed over the period March–April 1995 and recovered in March–April 1997 (Fig. 1). Good data was returned from 12 HEFRs, 17 IESs, and 17 current meters on seven moorings. Conductiv-ity–temperature–depth (CTD) profiles were ob-tained in the SAFDE region on eight cruises during the 1990s, four of which were during the SAFDE time period. The present study focuses on the measurements made by those IESs and HEFRs which were located within the main array, consisting of 16 IESs and 7 HEFRs. Also note that the temperature and pressure pair measure-ments from 300 to 1000 m on the easternmost current meter mooring (Fig. 1) were used to develop a synthetic IES record and fill a gap in the IES array following the methods of Meinen and Watts (2000).

An IES is about 0.6-meter tall and is moored about 1 m off the ocean bottom. It transmits a 10 kHz sound pulse and measures the time (τ) for the pulse to travel to the ocean surface and back (Watts and Rossby, 1977; Chaplin and Watts, 1984). Using historical hydrography from the region of study, characteristic relationships be-tween τ and other oceanic variables (e.g. tempera-ture, salinity, specific volume anomaly) can be developed and combined with the IES measured τ to provide full water column profiles of these variables (Meinen and Watts, 2000; Watts et al., 2001). The characteristic relationships are referred to as the "Gravest Empirical Modes", or GEMs, and there are separate GEM representations for temperature, salinity, and specific volume anom-aly. Vertically integrating the specific volume anomaly profiles provides profiles of geopotential height anomaly, which when differenced horizon-tally between neighboring IESs yield profiles of the relative velocity using the geostrophic (dynamic)
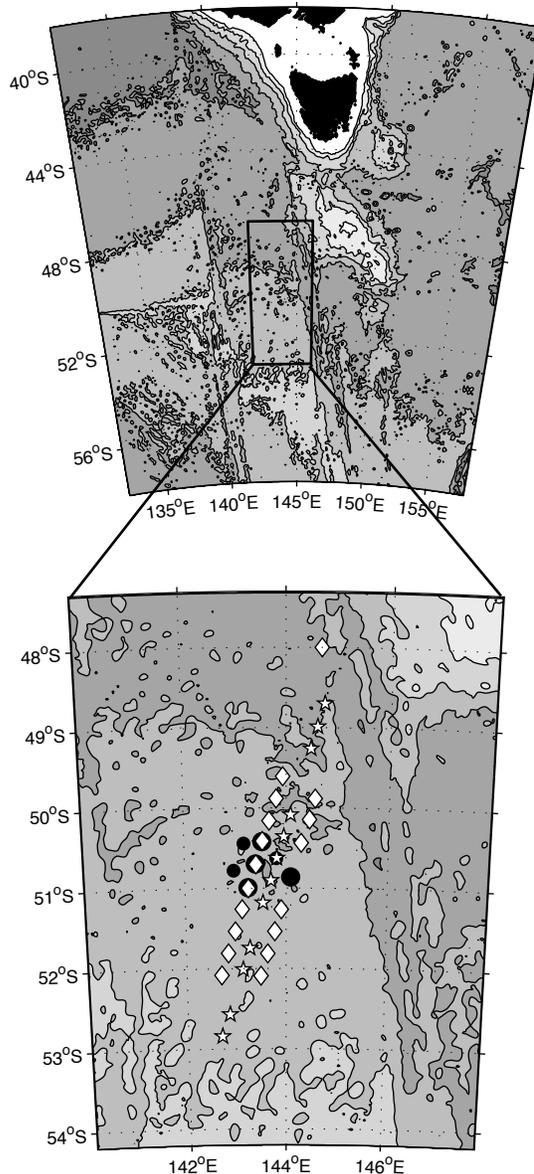
Fig. 1. Location of the SAFDE array. White diamonds, white stars, large black circles, and small black circles indicate IES, HEFR, tall current meter mooring, and short current meter mooring locations, respectively. Bottom topography, from Smith and Sandwell (1997), is denoted by gray shading at a contour interval of 1000 m. Black areas indicate land. Most of the SAFDE array region is 3000–4000 m deep.

method. Watts et al. (2001) present a detailed application of the GEM methodology to the SAFDE data set and provide a discussion of the

dynamical implications of the GEM fit to the raw hydrographic data.

The HEFR measures the horizontal electric field induced by the ions in seawater moving through the magnetic field of Earth (Sanford, 1971; Chave and Luther, 1990; Luther et al., 1991). Because seawater is conductive, the electric fields short out in the vertical and as a result the field measured by the HEFR represents the vertical mean of the horizontal field induced by the moving water. With proper calibration, this electric field is interpreted as the vertical mean horizontal water velocity. The HEFR measurements are then used to reference the relative velocity profiles determined by the IES/GEM methodology. As a result, time series of full-water-column absolute velocity profiles are obtained. The calibration of the HEFR in SAFDE is presented in Chave et al. (submitted for publication). The development of the characteristic hydrography relationships (GEM fields) and the combination with IES measurements followed the methods presented in Meinen and Watts (2000). The complete details of how the SAFDE IES and HEFR measurements were combined to provide daily (noon UT) time series of absolute velocity profiles have been presented in Meinen et al. (2002). That paper also presents a direct comparison between the absolute velocities measured by a current meter at a nominal depth of 2000 m and the HEFR + IES absolute velocities at the same site (HEFR 9, sixth star from the top in Fig. 1); the rms differences were 2.5 cm s^{-1} for the zonal currents and 1.7 cm s^{-1} for the meridional currents.

3. Motivation and methods

The motivation for describing strong oceanic currents in a stream coordinates reference frame, as opposed to Eulerian, has been widely discussed (Halkin and Rossby, 1985; Hall, 1986, 1989; Rossby, 1987; Hogg, 1992; Johns et al., 1995; Bower and Hogg, 1996; Kontoyiannis, 1997; Meinen, 2001). The analysis impediments arising from averaging in an Eulerian coordinate system result from two facts: first, the cores of strong oceanic currents shift laterally relative to the fixed

earth; second, the cores of the currents change direction relative to fixed geographic coordinates. Both of these facts lead to significant difficulty in interpreting and making dynamical inferences from measurements of fronts and their highly sheared currents using instruments moored at fixed locations.

The location of the SAFDE array was chosen to coincide with the WOCE SR3 repeat hydrography line. This line has been repeatedly occupied over the past decade (Rintoul and Sokolov, 2001), and it is one of the few places where data on the ACC has been collected regularly over a fairly long period of time. The western line of IESs (Fig. 1) is along the SR3 line, and the HEFR line is about 30 km east on a parallel track. Prior to SAFDE, data collected along the SR3 line have consisted principally of hydrographic sections, from which are determined profiles of the component of the relative velocity perpendicular to the section (e.g. Rintoul and Sokolov, 2001). For comparison, the time mean of the absolute velocity component perpendicular to the HEFR line is presented in Fig. 2 (upper panel). The section shows two current cores, a relatively strong eastward flow at the southern edge of the array (left side of figure), and a much weaker eastward flow in the northern part of the section. Based on the altimetry results of Gille (1994), not shown, these flows appear to correspond to the Polar Front (PF) and SAF, respectively[1]. Observing stronger PF velocities than for the SAF runs counter to expectations (e.g. Rintoul et al., 2001): however, this is an artifact of the orientation of the HEFR (and SR3) line. Because the HEFR and IES array can provide both components of the velocity, we can look at the component of the velocity parallel to the HEFR line as well (Fig. 2, lower panel), something which the earlier hydrography-based sections could not do. The velocity component parallel to the HEFR line indicates fairly strong northward flow in the same region as the fairly weak SAF

---

[1] N.B. Some hydrographic sections from this region have suggested that the southern of these two fronts is not actually the PF (e.g. Rintoul and Sokolov, 2001). We make no claims based on our SAFDE data whether this is or is not the real PF; we use the name here only to help distinguish between the northern and southern fronts.
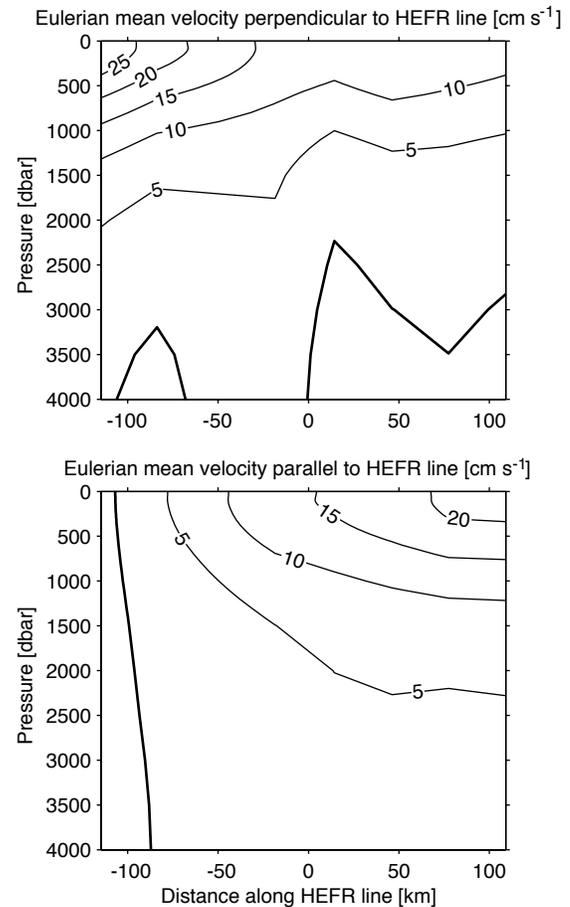

Fig. 2. Eulerian time-mean absolute velocity observed during the 701 day SAFDE. Velocity components perpendicular to the HEFR line (upper panel) and parallel to the HEFR line (lower panel) are shown. Velocities are in cm s^{-1}, bold contour denotes zero velocity.

flows indicated in Fig. 2 (upper panel). The parallel flow associated with the PF is quite weak, indicating that in the mean the PF crossed the HEFR line nearly perpendicularly, unlike the SAF.

3.1. Choosing a stream coordinates origin

The meandering of the SAF and PF temperature and current fields results in the overly broad, smooth mean currents shown in Fig. 2. Those currents provide little information about the

"synoptic" structure of the SAF. (Because the PF is only captured within the southern end of the array on a sporadic basis, this paper focuses on the SAF.) In order to determine the stream coordinates mean structure of a current, the first step is to determine a definition for its center (the origin of our new Cartesian coordinate system fixed to the current). One of the most commonly used definitions is that of a particular isotherm crossing a specific pressure surface (e.g. Johns et al., 1995). Other studies have used the midpoint between an isotherm crossing two isobars (Rossby, 1987), a particular specific volume anomaly occurring on a pressure surface (Phillips and Rintoul, 2002), etc. An important consideration with regards to this determination is how the cross-stream distance is going to be determined. If a "frozen-field" baroclinic structure is going to be assumed (that is, a time-invariant cross-stream pycnocline structure), then there is no requirement that the origin for the stream coordinates be the center of the current. Such an assumption will not be made at this time, so a stream coordinates origin will be chosen which is at the approximate center of the current.

The stream coordinates origin is defined here as an isotherm crossing a particular pressure level. In order to determine the isotherm which was most often found at the middle of the main thermocline, the depth of the maximum vertical gradient of temperature within the main thermocline is defined to be the middle of the thermocline and the relationship between temperature and the vertical gradient of temperature was studied using the 183 CTD profiles obtained within the SAFDE region (Fig. 3). Based on these comparisons it is apparent that the 6°C isotherm is at the middle of the main thermocline more often than the neighboring isotherms. For this reason 6°C was chosen for the isotherm to use for the stream coordinates origin. In order to determine the pressure surface at which the 6°C isotherm crossing would define our origin, the same hydrography was used to determine the vertical distribution of the 6°C isotherm observations (Fig. 4). Since the thermocline's depth across the SAF is similar to a hyperbolic tangent profile, and since there is a reasonably even distribution of CTDs on either
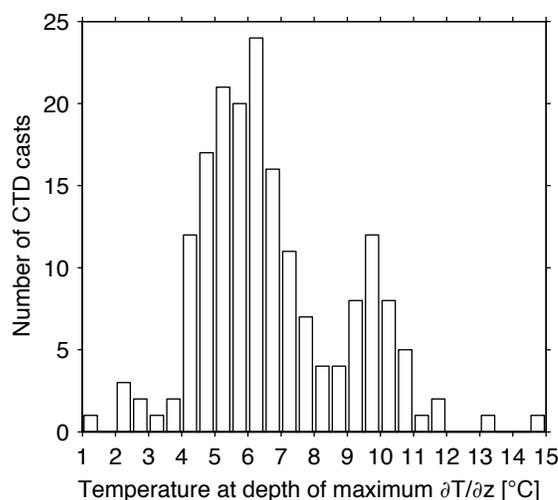

Fig. 3. Histogram showing the temperature at the depth of the maximum vertical gradient of temperature within the thermocline from a set of 183 CTDs obtained in the SAFDE region.
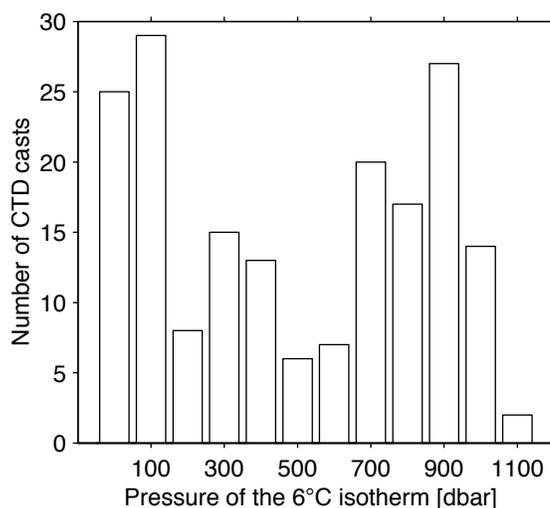

Fig. 4. Histogram of the observed pressure of the 6°C isotherm from a set of 183 CTDs obtained in the SAFDE region.

side of the front, one would expect a bi-modal distribution with most observations of the 6°C isotherm depth occurring either at the shallower depth common on the south side of the SAF or at the deeper depth common on its north side. The center point between these two maxima should represent the middle of the 6°C isotherm's

excursion across the front. Based on the CTD data, the pressure level at which this minimum occurs is about 500 dbar. Accordingly, the origin of our stream coordinates system is defined as the location where 6°C crosses 500 dbar.

3.2. Defining cross-stream location

Once the stream coordinates origin has been defined, all of the velocity measurements must be located relative to the daily varying origin location. Fig. 5 shows daily maps of the depth of the 6°C isotherm (Z_6) within the array, illustrating some of the different paths which the SAF took across the array during the experiment. These maps of isotherm depth were produced by combining optimally interpolated (OI) (Bretherton et al., 1976) IES data with GEM hydrographic characteristics to determine the vertical profile of temperature (Meinen and Watts, 2000; Meinen et al., 2002). The center of the SAF front, where $Z_6 = 500$ dbar, is denoted by the bold black line. During the 2-year experiment, the SAF crossed the array at nearly every direction of the compass: towards the east (e.g. October 4, 1996); towards the north (e.g. January 6, 1996); and towards the south (e.g. December 4, 1995). At times when there were large meanders or rings in the front there was even a significant westward component to the flow (e.g. August 3, 1996). Furthermore, because of these same meanders and rings, the SAF at times crossed the array in more than one location. During the 701 day experiment there were 57 days with two or three crossings of the HEFR line, and there were 38 days when there was no crossing of the SAF on the HEFR line. This emphasizes the need to move away from an Eulerian description of the flow along the SAF and towards a stream coordinates description.

The next step in converting to stream coordinates, after defining the origin (core) location, is to determine how far from the core each of the current measurements was obtained. A number of different methods have been developed for determining this distance; these different methods fall into two basic categories. In experiments where only a few moorings were deployed, it was assumed that there was no temporal variability

of the baroclinic structure, and "frozen-field" cross-sections of temperature (e.g., Hall, 1986) or specific volume anomaly (e.g., Phillips and Rintoul, 2000, 2002) were developed to determine the cross-stream location given a particular observation of temperature or specific volume anomaly at a specific depth/pressure. Fig. 6 illustrates two possible frozen-field cross-sections which could be used for the SAFDE region. The well-known problem with this technique is that it does not allow for baroclinic variability over time, although depending on data availability such an assumption may be the only available path for analyzing the data[2].

When gridded data from an array of IESs are concurrently available, a different method can be used to determine the cross-stream location of the velocity measurements. The distance between the velocity measurement location and the location of the contour which describes the path the core takes through the array, such as those shown by bold lines in Fig. 5, can be determined directly. Fig. 7 schematically illustrates the method for determining distance. Each circle in the figure represents a location where velocity measurements were made on this hypothetical day. The thick gray line represents the path which the core of the current is taking through the array, while the dotted line represents the boundaries of the OI mapping region of the IES data. The closest point of approach on the path provides the distance between the measurement site and the core of the SAF, as long as the line between the measurement site and the closest point is normal to the tangent of the path (thin black lines). If no perpendicular can be drawn (thin black dashed lines), it suggests that the closest point of approach of the core is outside of the IES array, and as such the velocity measurement for that particular site and day cannot be accurately used in determining the stream coordinates structure. Note that while the

---

[2] The original stream coordinates method presented in Hall and Bryden (1985), and used in modified form by Phillips and Rintoul (2002), involved averaging first in temperature bins and used the 'frozen field' only for converting the mean velocity values onto a distance axis. Because averaging is a linear process that method is mathematically identical to the 'frozen field' method applied to the daily data as presented herein.

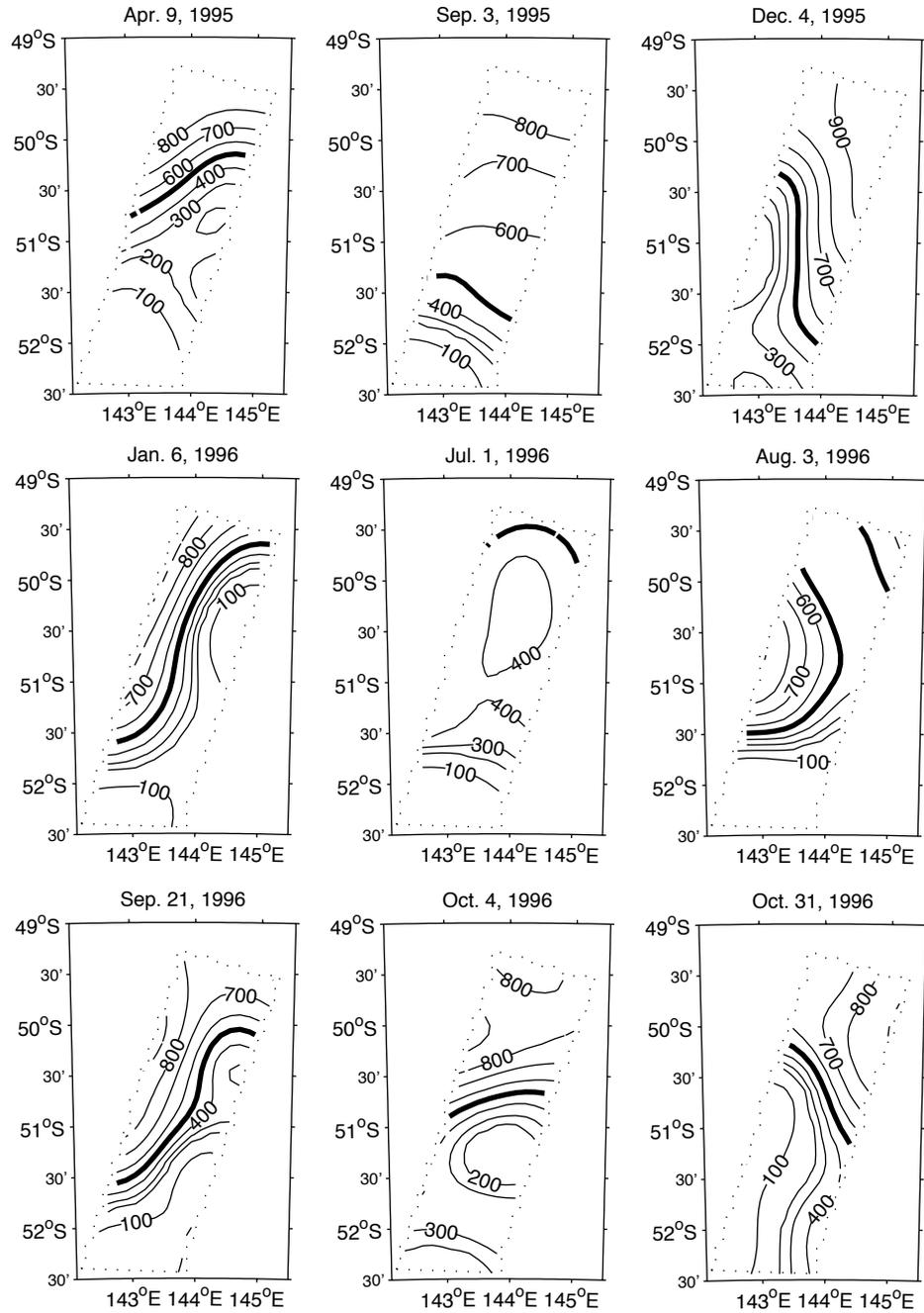Fig. 5. Examples of OI maps of the 6°C isotherm depth (Z_6) on nine selected days during SAFDE. Contour values are pressure in dbar. The 500 dbar contour, denoted by the bold line, is our definition of the SAF core. Dotted line indicates the border of the OI mapping region.
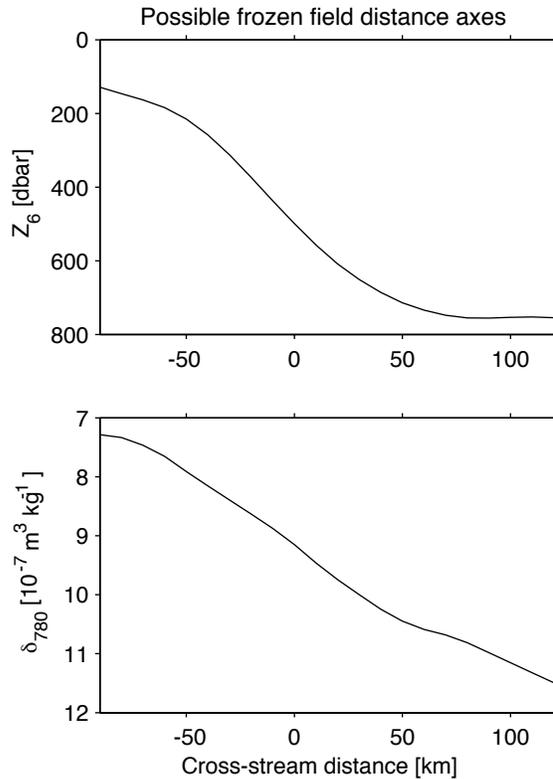
Fig. 6. Possible frozen field distance axes; upper panel shows a canonical cross-stream section of the $6°C$ isotherm pressure, while the lower panel shows a cross-section of the specific volume anomaly at 780 dbar. The latter is similar to the frozen-field axis used by Phillips and Rintoul (2002).

schematic illustration in Fig. 7 showed the path as a straight line, the path is more often curved like the examples shown in Fig. 5; however, this is not a hindrance to the method described above.

The main advantage to determining the cross-stream distance in this manner is that no assumptions regarding baroclinic time-invariance need to be made. As such, the observations from this study can be used to explore the time variability of the baroclinic structure of the SAF. Fig. 8 (upper panel) illustrates the wide variety of Z_6 cross-sections observed during the 2 year SAFDE. The Z_6 at the HEFR sites were determined by vertically interpolating the temperature profiles estimated for each HEFR site on each day from the OI gridded IES τ values and the temperature GEM field. On each day the maximum number of
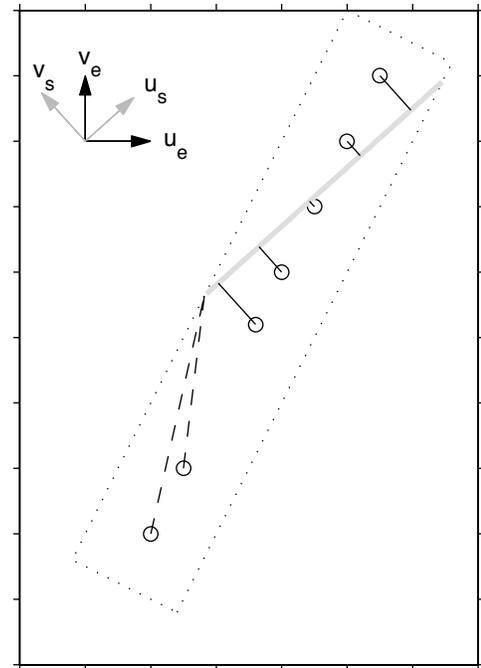

Fig. 7. Schematic demonstrating the OI method for determining cross-stream distance and downstream angle. The bold gray line represents the core of the current, while the dotted line represents the boundary of the OI mapping region (similar to Fig. 5). Open circles represent HEFR sites, and thin black lines are the perpendicular lines drawn between the HEFR sites and the closest point on the idealized SAF core. Dashed lines demonstrate that perpendicular lines cannot be drawn between the two southernmost HEFRs and the closest point on the core contour on this particular day. The black pair of arrows indicate east (u_e) and north (v_e) directions in geographic coordinates, while the gray pair of arrows demonstrates downstream (u_s) and cross-stream (v_s) for this idealized case. Because in reality the core contour would not generally pass through the mapping region as a straight line, the actual orientation of downstream would be determined independently for each HEFR site based on a tangent line to the core at the point where the perpendicular line (thin black lines) intersected the core (bold gray line).

Z_6 estimates possible was seven (one at each HEFR site), so to obtain more complete cross-sections spatial gaps in cross-stream location of up to 50 km were interpolated. Only days which had at least four Z_6 measurements, and where there were measurements spanning the core, were plotted. The mean Z_6 cross-section is also shown.
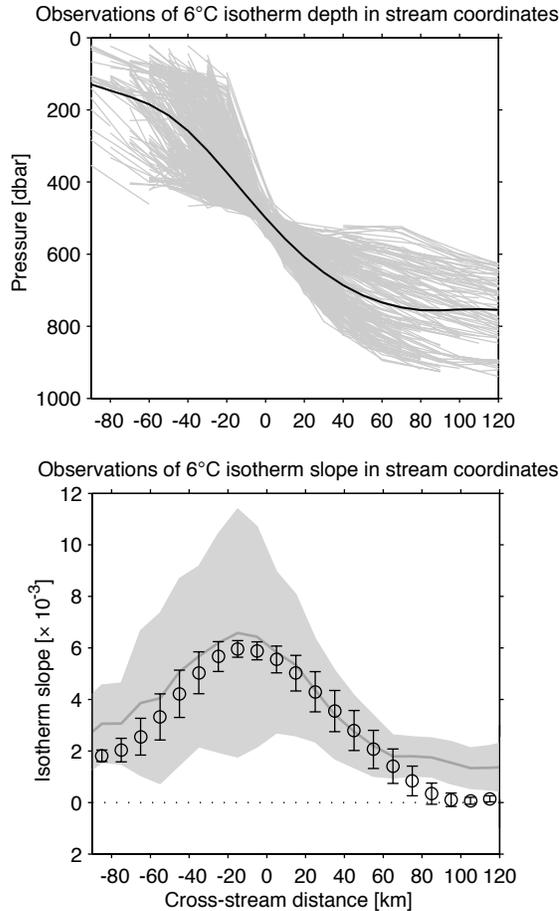
Fig. 8. Upper panel: The observed cross-sections of 6°C isotherm depth (gray lines) during SAFDE, see text for details of determination. The bold black line represents the mean of the gray lines. Lower panel: The gray line and band represent the mean and range of the observed cross-stream slopes of the 6°C isotherm depth (mean plus and minus one standard deviation). The open black circles and associated error bars represent the scatter due to subsampling errors (see the text for detail).

The lower panel of Fig. 8 demonstrates the variability in Z_6 slopes with the gray line and band, which represent the mean slope plus or minus one standard deviation. Near the center of the SAF this range of observed slopes represents approximately a factor of 2 deviation from the mean in either direction (smaller or larger).

The variability shown in Fig. 8 suggests large baroclinic changes occurred during the 2-year experiment. It could be argued, however, that the

variability in the slope in Fig. 8 results from the interpolation needed to obtain cross-sections from only 4–7 observations of Z_6 on a given day. To confirm that this observed variability in slope is not due simply to the limited sampling and interpolation necessary to fill gaps between measurements, 7100 random four point sub-samples of the mean observed Z_6 cross-section were made (i.e. over 10 times the number of actual daily samples). For each four point sample, gaps smaller than 50 km were filled and only samples which had "observations" on either side of the core were used. The mean and standard deviation of the resulting slopes are shown in the lower panel of Fig. 8. The variability induced by sampling is much smaller than the observed slope variability, demonstrating that the majority of the variability shown by the gray area must be actual ocean variability. The mean values from the random samples are slightly lower than the mean of the observed Z_6 slopes because random sampling and interpolation can only smooth the mean curve.

Fig. 8 suggests that assuming no temporal variability of the baroclinic structure for the flow along the SAF would result in significant errors in determining cross-stream location. In order to quantify this error, the specific volume anomaly along 780 dbar (δ_{780}) cross-section from Fig. 6 was combined with the estimated δ_{780} on each day at the HEFR sites to determine the cross-stream location which would have been obtained under the assumption of no baroclinic temporal varia-bility. The cross-stream distance estimated in this manner is compared (Fig. 9a) to the distance determined using the OI mapped Z_6 field as discussed previously. The differences between the two estimates of distance are small near the core, but they increase rapidly further from the core (Fig. 9b). While the two quantities roughly follow the 1-1 line, the scatter is quite large. Fig. 9b details the root-mean-square (RMS) differences within 10 km wide bins. At 20 km from the core on either side of the front the RMS differences exceed 10 km, and by 40 km from the core the differences exceed 20 km, demonstrating the large errors which would result from assuming a time-invariant Z_6 cross-section.
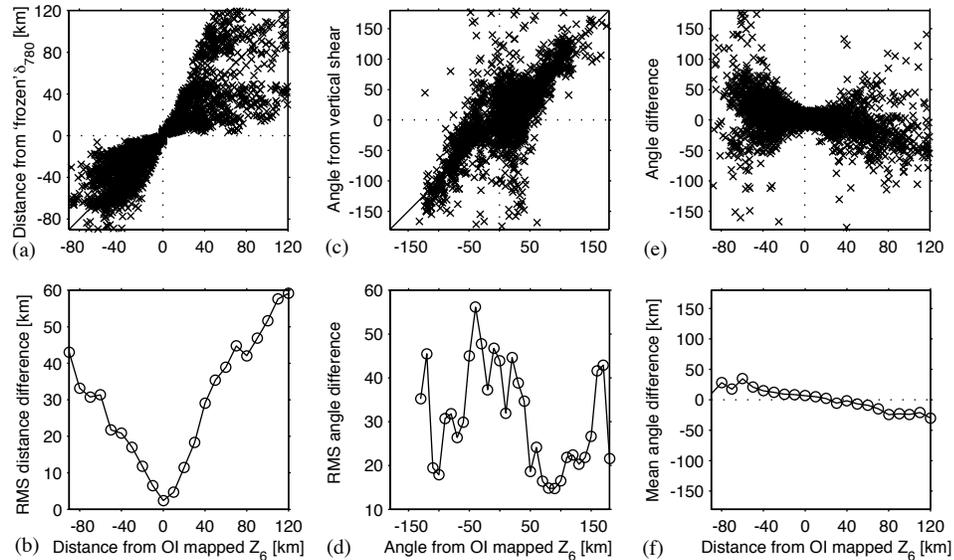
Fig. 9. Stream coordinates methods: (a) comparison of cross-stream distance determined using frozen-field distance versus using OI mapped 6°C depths; (b) RMS distance differences from (a) determined in 10 km wide bins; (c) comparison of downstream angle determined using the direction which maximizes the vertical shear of horizontal velocity versus the downstream angle determined from the OI mapped 6°C depths (0° represents East); (d) RMS differences from (c) determined in 10° wide bins; (e) difference in angle from (c) as a function of cross-stream distance; (f) mean angle differences from (e) averaged in 10 km wide bins. All quantities calculated from SAFDE data.

These errors in stream coordinates distance will have essentially no effect at the core of the SAF, but away from the core they tend to smooth the cross-section. To demonstrate this effect, an idealized along-stream velocity cross-section based on a Gaussian (normal) function was created (Fig. 10a). The idealized cross-stream flow was based on a hyperbolic tangent, which simply simulates a divergent current. To simulate the effect of distance errors on the idealized cross-section, a series of random values was generated for each distance grid point along the cross-section. The magnitude of the random values was set so that the RMS value of the random values was equal to the corresponding value from a linear fit to the RMS differences shown in Fig. 9b. The number of random values at each grid point was given by a linear model with 300 samples in the central bin and dropping to 20 by ±120 km, simulating the real distribution of observations. The random distance errors, combined with the 'correct' distance for a particular bin, were used to extract a "time series" of velocities from the

idealized cross-sections. The resulting erroneous simulated velocity values were then averaged and the difference between that average and the idealized velocity at that distance grid point provides an estimate of the impact of using a time-invariant baroclinic structure for determining cross-stream distance. The resulting mean velocity cross-section agrees well with the correct cross-section near the core of the current; however, significant smoothing and increased transport results near the flanks of the current (Fig. 10a). Based on the realistic values used in this simulation, the transport which would be calculated under the assumption of no baroclinic variability would be about 12% too large. Furthermore, energetics studies frequently require estimates of the cross-stream gradient of along-stream velocity (e.g. Kontoyiannis, 1997); it is evident from Fig. 10a that estimates of that gradient will be weakened on the flanks of the current and the current will also appear artificially wide. While the assumption of no baroclinic variability is indeed the only way to obtain stream coordinates
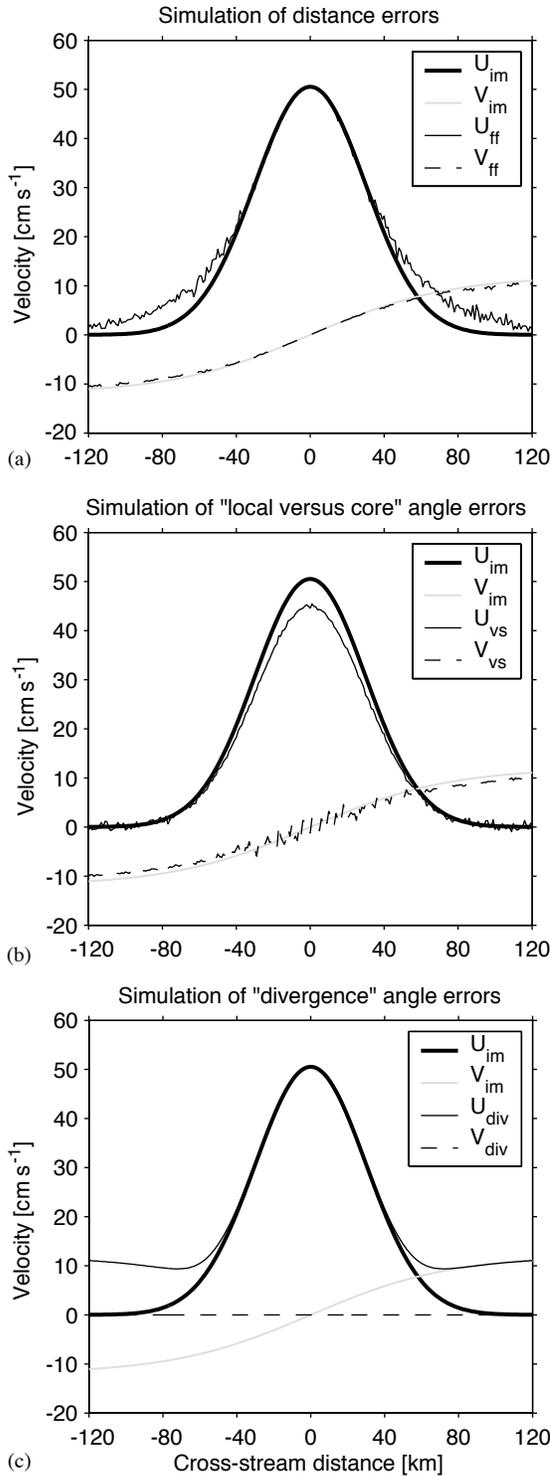
information from a limited number of moorings, the results shown here suggest that results obtained from such calculations must be interpreted with caution, at least in the SAF.

3.3. Determining downstream direction

For the final step in moving into stream coordinates, rotating the velocities, there also are basically two methods which have been applied in the past: defining the downstream direction as the direction which locally maximizes the vertical shear of the horizontal velocities; and using other horizontally gridded information, such as thermocline depth determined from IESs, to determine the downstream direction (Johns et al., 1995; Bower and Hogg, 1996). The former method must be used when data from just a few moorings are available, the latter can be adopted only when there is a large array of moorings. Johns et al. (1995) describe both methods in some detail in a stream coordinates application to current meter mooring measurements in the Gulf Stream near 68°W. In that study the vertical shear method was used whenever the difference between current meter measured velocities at 400 and 1000 m exceeded 5 cm s^{-1}. When the shear was smaller, the direction was determined by following the path of the 12°C isotherm crossing 400 dbar through the array. Johns and coauthors calculated the 12°C isotherm depth field from the measurements of an array of IESs which surrounded and overlapped the current meter mooring array.

Fig. 10. Simulating the errors induced by using the frozen-field cross-stream distance method and/or the vertical shear method of determining downstream direction. For all panels the bold black (along-stream) and gray (cross-stream) lines represent a simple idealized model velocity cross-section at a particular depth. The thin lines simulate the cross-sections which would be obtained under the following situations: (a) using the frozen field distances but the OI method for determining the downstream angle; (b) using the OI method distances but including a random downstream direction error due to using the local vertical shear for determining the downstream angle; (c) using the OI method distances but rotating the cross-stream flows into along-stream to simulate an angle bias error similar to what is shown in Fig. 9f.

There are two potential problems with using the vertical shear method for finding the direction of downstream. First, the presence of eddies and rings within and near the current suggests that the direction of strongest shear at a particular mooring location may not be parallel to the downstream direction some distance away at the core of the current. This represents a random angle error which can occur anywhere across the current. Second, the presence of recirculation gyres on either side of a current, well documented in the Gulf Stream (Hogg, 1992) and likely present around the ACC as well, indicates that away from the current core axis there is either a divergent component or a convergent component to the water velocity due to the divergence or convergence of the recirculation cells. This implies that the direction of largest shear, at locations away from the core axis, may not be parallel to the core if there is a baroclinic component to the recirculation cells. The result would be a bias with all observed angles on one side of the current having errors of one sign and all observed angles on the other side of the current having errors of the opposite sign.

Consider first the former (random angle) problem. Fig. 9c shows a comparison of the downstream angle as determined from the velocity shear method to the angle as determined from the OI mapped Z_6 field as shown in Fig. 7. There is a suggestion of a 1-1 correspondence in general; however the scatter is quite large. There is no particular pattern to the differences (Fig. 9d), which is not surprising considering the possible combinations of a widely varying downstream direction (e.g. Fig. 5) with randomly located eddies and rings. The effect of a random angle error on an idealized current in the presence of a cross-stream divergence is mainly a reduction in the along-stream velocity in the core of strong velocities; the effect on the cross-stream velocities is roughly the same on a percentage basis, but given the smaller magnitude of the cross-stream flow the effects are primarily noted as a slight weakening of the mean divergence and the introduction of a small amount of noise (Fig. 10b).

A more diagnostic test is to look at the differences in angle as a function of cross-stream distance (Fig. 9e). While there is still a great deal of scatter in the individual observations, by bin averaging the observed distances a distinct biasing pattern emerges (Fig. 9f). This pattern is statistically significant at the 95% confidence level. For locations on the warm side of the SAF core (positive distances in Fig. 9f), the differences are negative, indicating that the shear method gives a downstream direction which is rotated counterclockwise of that given by the OI mapped values. For locations on the cold side of the front the result is the opposite. This suggests that by using the OI mapped Z_6 method the resulting cross-stream divergence will be larger than that which would be determined from the velocity shear method. By 50 km from the core this angle difference is 10–20°, which is quite significant. The effect of an angle bias error on the idealized along-stream current (Fig. 10c) is small near the core of the current, but it artificially increases the flows out near the flanks of the current. The cross-stream flows are zero if the entire cross-stream component is rotated into along-stream.

Bower and Hogg (1996) documented another danger of using the vertical shear method to determine downstream direction. Their Gulf Stream study found a curvature-dependent angle offset between the vertical shear and OI-mapped methods; the vertical shear method consistently demonstrated equatorward cross-stream flow when transitioning from a meander crest to a trough and poleward flow when changing from trough to crest. They pointed out that this flow is not related to inflow or outflow from recirculations outside of the Gulf Stream and as such the vertical shear method should not be used if assessing these convergences or divergences is a goal of the study.

3.4. Optimum method for defining stream coordinates

Herein follows the optimum conversion to stream coordinates as proposed in this study. For each day of the time series, Z_6 was contoured through the array using the IES data. Then, for each site on each day, the closest point on the $Z_6 = 500$ dbar contour was found and, if the line

between that point and the HEFR site was within $10°$ of perpendicular to a tangent to the contour, the point was defined as the location of the core for that HEFR site for that day. The distance between the two points was defined as the cross-stream distance (positive if the $6°C$ isotherm at the HEFR site was deeper than 500 dbar, negative if it was shallower), while the tangent to the contour line provided the direction of downstream for rotation of the velocities into along-stream and cross-stream components. This process was repeated for each of the seven HEFR within the main array, and then the processing continued on to the next day of the time series and the procedure repeated. For situations where the closest point on the contour was less than 3 km away from the HEFR site, the distance was set to 0 km and the tangent at the closest point provided the definition of downstream. For situations where the choice of a closest point was particularly ambiguous, such as when two points on the contour were nearly equidistant from the HEFR site, the data from that site on that day were not used in developing the stream coordinates mean.

Of the 4907 absolute velocity profiles (7 HEFR sites times 701 days), 3100 could be used in determining the stream coordinates mean. For the remaining profiles, their particular sites were located relative to the SAF core such that the closest approach of the SAF was either outside the IES array (see Fig. 7) or was ambiguously defined, and therefore the cross-stream location and downstream direction could not be determined. (Note that the frozen-field method and local vertical shear methods do not have these restrictions, and therefore can utilize all 4907 profiles. This does not lead to better results, as will be shown shortly.) The usable velocity estimates, as well as the temperature and salinity estimates at those sites as determined from the IES gridded τ values and the GEMs, were averaged in 10 km wide bins centered at 10 km intervals from the stream coordinates core. The resulting mean sections were smoothed slightly using a 40 km low-pass filter (second-order Butterworth filter passed both forward and back to avoid phase shifting) in order to facilitate the intercomparisons of the various sections (smoothing is not applied for dynamical

studies; see Meinen et al., submitted for publication). No vertical smoothing was applied. The number of velocity observations used in the stream coordinates averaging ranged from about 10 observation-days for the bins 150 km from the core to about 300 observation-days at the core. Only bins with at least 20 observation-days were considered to have useful means, which restricted the usable range to within 90 km on the cold side of the SAF and to within 120 km on the warm side of the front.

4. Results

Fig. 11 presents the stream coordinates mean along- and cross-stream velocity produced when the OI mapped Z_6 field is used for determining both the downstream direction and the cross-stream distance. The peak along-stream velocities are about 50 cm s^{-1} at the surface, and at 4000 dbar the peak velocities reach 2 cm s^{-1}. The along-stream velocities have a single peak, similar to other oceanic jets such as the Gulf Stream (Johns et al., 1995) and the North Atlantic Current (Meinen, 2001). Those other currents, however, clearly have a more asymmetric structure and an equatorward displacement of the velocity maximum with increasing depth, neither of which is very evident in the SAF. The cross-stream flow is divergent both baroclinically and (weakly) barotropically, with peak velocities of $8–10 \text{ cm s}^{-1}$ near the surface and near bottom velocities of about $1–2 \text{ cm s}^{-1}$. [N.B. barotropic is defined as the near bottom velocity following Fofonoff (1962).] The equatorward flow on the warm side of the SAF is consistent with the anticyclonic recirculation north of the front as proposed by Rintoul et al. (2001) on the basis of repeated hydrographic sections; however, the poleward flow on the cold side of the SAF does not correspond in an obvious way to the circulation picture proposed by those authors. The mean absolute transport along the SAF, integrated from the bottom to the surface and between the 10 km wide bins centered at -90 and $+120$ km, was 75 Sv (Sv: $10^6 \text{ m}^3 \text{ s}^{-1}$).

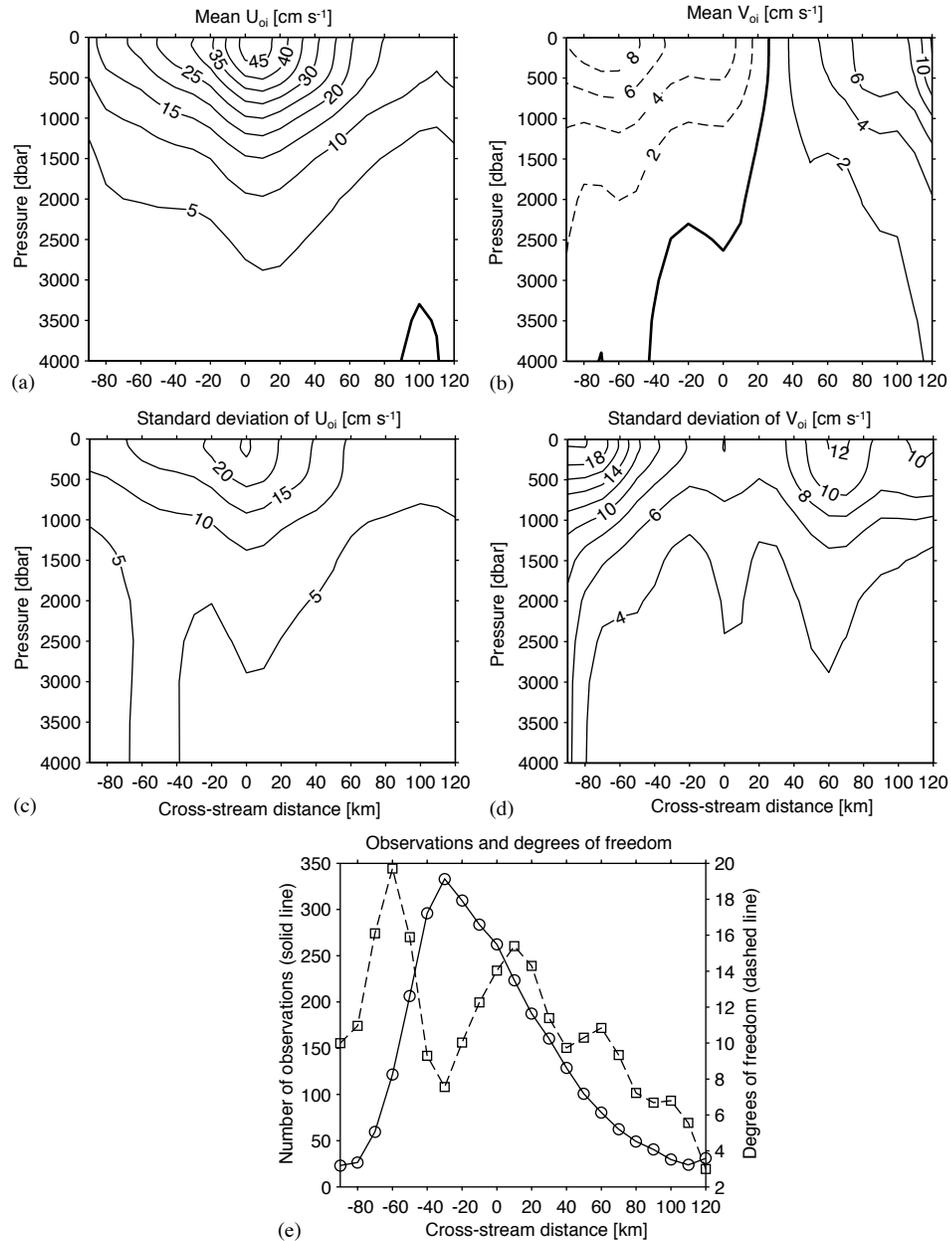Consider next the results of determining the stream coordinates mean using the 'correct'

Fig. 11. (a) The along-stream mean current section from stream coordinates using the OI method for both downstream direction and cross-stream distance definitions; (b) the cross-stream mean current section from stream coordinates using both OI stream coordinates definitions; (c) the standard deviation of the along-stream current; (d) the standard deviation of the cross-stream current; (e) solid line shows the number of absolute velocity profile observations used in the averaging within each 10 km bin, dashed line shows the estimated number of degrees of freedom within each 10 km wide bin. In panels (a)–(d) the solid contours indicate positive flow, dashed contours indicate negative flow, and the bold contour indicates zero flow. Contours are in cm s^{-1}. Note along-stream and cross-stream currents have different contour intervals.

rotation angle as determined from the OI mapped Z_6 field but estimating the cross-stream distance using the 'frozen-field' structure of δ_{780} (Fig. 12). The resulting stream coordinates mean along-stream velocity displays two maxima in the upper 1000 dbar. The current structure is significantly different from that of the 'correct' section shown in Fig. 11, with a smearing of the velocity signals
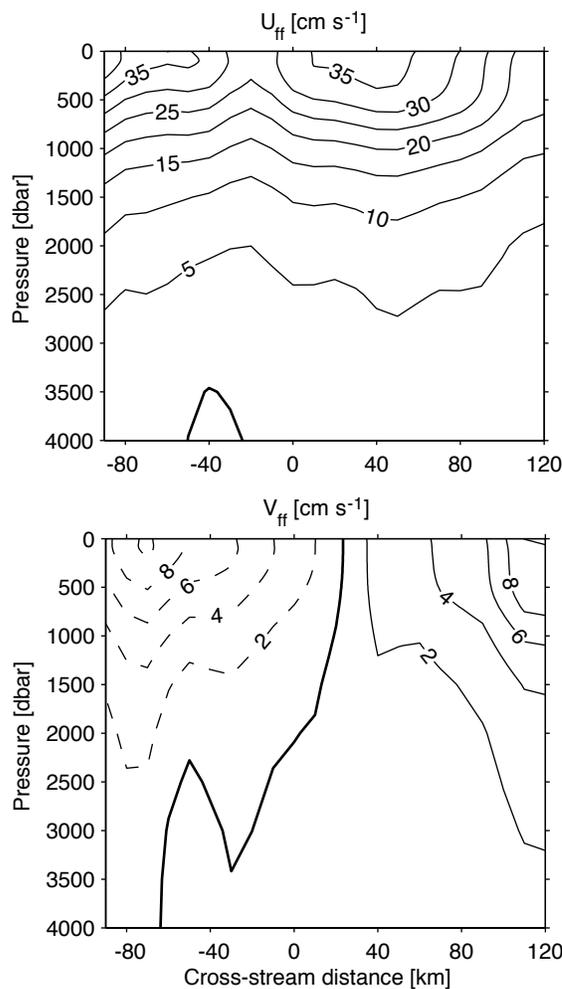

Fig. 12. The along-stream (upper panel) and cross-stream (lower panel) stream coordinates mean sections obtained using the OI method for determining downstream direction but the frozen field method for determining cross-stream distance. Solid contours indicate positive flow, dashed contours indicate negative flow, bold contour indicates zero flow. Contours are in cm s^{-1}. Note along-stream and cross-stream velocities have different contour intervals.

over larger horizontal distances and a 30 km northward shift of the deep velocity maximum. The cross-stream flow, by contrast, is fairly similar between the sections shown in Figs. 11 and 12. This is consistent with the idealized results shown earlier (Fig. 10a).

If instead the stream coordinates mean is determined using the 'correct' OI mapped cross-stream distances but using the local vertical shear for downstream direction, the resulting along-stream flow (Fig. 13) is very similar to the 'correct' estimates from Fig. 11 near the SAF core. Away from the core, however, the use of the local vertical shear direction results in stronger along-stream flows. This is to be expected because the cross-stream flows in Fig. 11 are rotated into along-stream flows in Fig. 13. The cross-stream flows in Fig. 13 are generally very small, with no significant baroclinicity in the cross-stream flow because of the direction definition. The resulting along-stream transport from Fig. 13 exceeds that of Fig. 11 by 10%, while the cross-stream transports are obviously much smaller when the vertical shear is used for the direction.

A final comparison is made to the stream coordinates mean velocity sections which were obtained by using the 'frozen-field' distances and the vertical shear directions, e.g. the 'wrong' methods for both distance and direction (Fig. 14). The general patterns of Figs. 12 and 13 are evident in Fig. 14: multiple along-stream velocity peaks, little cross-stream flow, broad and large along-stream transports. With limited data, such as a few current meters, and no OI mapped field of IESs, the only stream coordinates mean section which could have been obtained for the SAF in this region would be similar to the one shown in Fig. 14. However, because of the availability of the OI mapped Z_6 fields for deriving cross-stream distances and rotation angles, it has been possible to document that the 'true' stream coordinates section is that shown in Fig. 11. The significant differences between the two sections (Figs. 11a, b and 14) raise questions about whether determining the stream coordinates mean from a limited number of moorings is a viable approach. Extracting cross-sections at several depth levels from each of the sections shown in Figs. 11–14
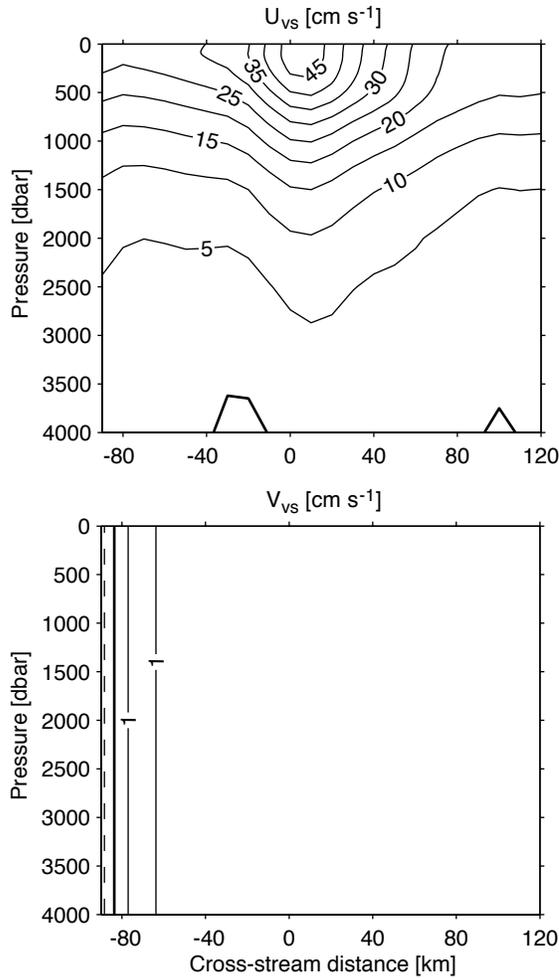
Fig. 13. The along-stream (upper panel) and cross-stream (lower panel) stream coordinates mean sections obtained using the OI method for determining cross-stream distance but the vertical shear method for determining downstream direction. Solid contours indicate positive flow, bold contour indicates zero flow. Contours are in cm s⁻¹. Note along-stream and cross-stream velocities have different contour intervals.
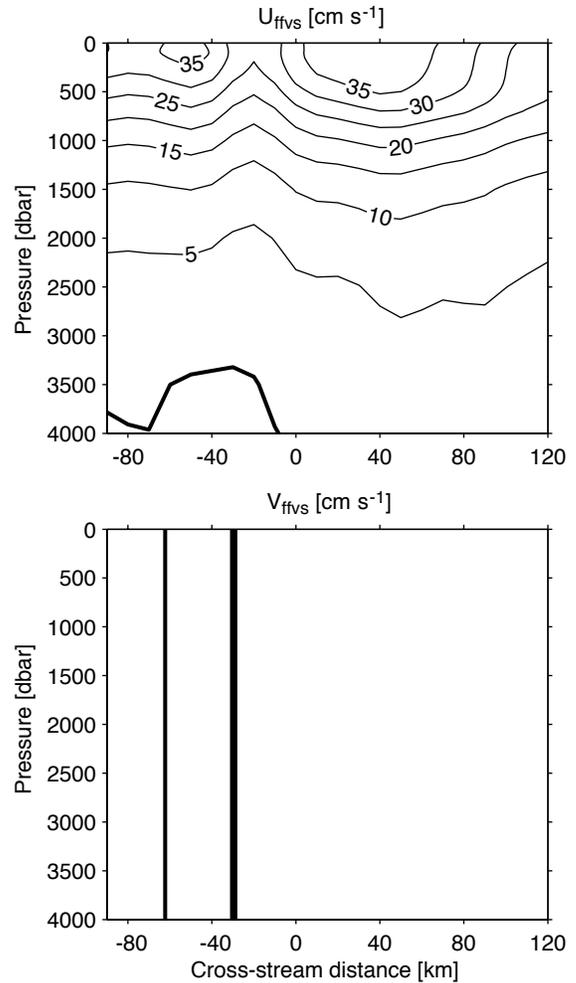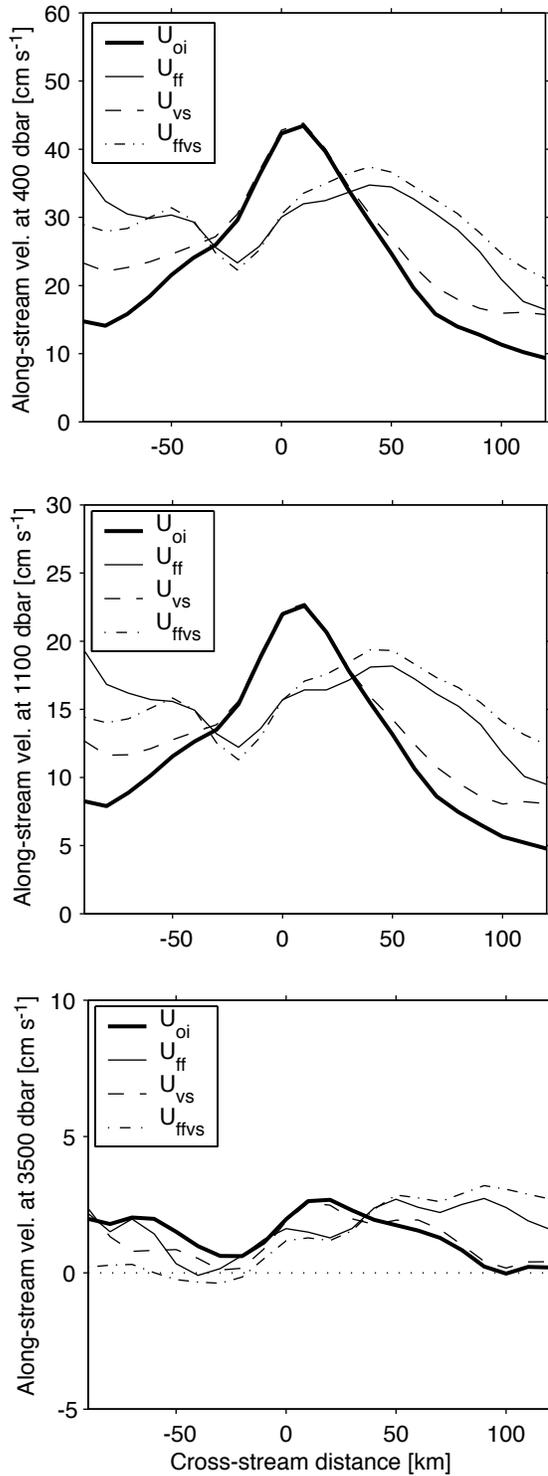
Fig. 14. The along-stream (upper panel) and cross-stream (lower panel) stream coordinates mean sections obtained using the vertical shear method for determining downstream direction and the frozen-field method for determining cross-stream distance. Solid contours indicate positive flow, bold contour indicates zero flow. Contours are in cm s⁻¹. Note along-stream and cross-stream velocities have different contour intervals.

emphasizes further (Fig. 15) that the use of either the 'frozen-field' method of determining cross-stream distance or the use of the local vertical shear of horizontal velocity for determining the downstream direction results in inaccurate estimates for the along-stream velocity means in the SAF. It will be shown shortly that these differences can have important impacts on the dynamical interpretation of the stream coordinates mean section.

4.1. Optimum method results

Fig. 11a presents the 'correct' mean along-stream absolute velocity for the SAF, along with the standard deviation (Fig. 11c) and the number of daily velocity profiles which were used within each 10 km wide averaging-bin (Fig. 11e). The standard deviations of the along-stream velocities demonstrate that the strength of the ACC flow

Fig. 15. A comparison of the stream coordinates mean velocities from Figs. 11–14 at three depth levels; 400, 1100, and 3500 dbar (top, middle, bottom). Legend shows to which mean section each line corresponds; "oi" indicates the OI method was used for both downstream angle and cross-stream location (Fig. 11), "ff" indicates OI method was used for downstream direction but frozen-field method was used for cross-stream location (Fig. 12), "vs" indicates OI method was used for cross-stream location but vertical shear method was used for downstream direction (Fig. 13), "ffvs" indicates frozen-field method was used for cross-stream location and vertical shear method was used for downstream direction (Fig. 14).

along the SAF changes significantly, with the core at the surface having a standard deviation of about $25\ \mathrm{cm\,s^{-1}}$. Since the effect of meandering is removed from the stream coordinates reference frame, the baroclinic nature of the standard deviations suggests that there was a significant amount of baroclinic variability observed during the experiment, consistent with Fig. 8.

The cross-stream mean absolute velocities (Fig. 11b) and standard deviations (Fig. 11d) demonstrate that the divergence, with northward flow north of the core and southward flow to the south, was quite variable during the experiment. The mean divergence pattern is statistically significant, however, even though the meander patterns (and hence the curvature) were so variable during SAFDE (e.g. Fig. 5).

Before continuing, a brief discussion of the measurement accuracy of these velocity estimates is in order. Meinen et al. (2002) quantify the accuracy in the absolute velocities derived from the IES and HEFR measurements to be 8, 6, 4, and $3\ \mathrm{cm\,s^{-1}}$ for pressures of 300, 600, 1000, and 2000 dbar, respectively. These one standard deviation error bars are for the daily velocity measurements and they were determined by comparison with several current meters involved in SAFDE as well as other independent data. In order to determine the accuracy of the stream coordinates mean values shown in Fig. 11 an estimate of the degrees of freedom must be made. Johns et al. (1995) showed that the number of degrees of freedom in a stream coordinates reference frame was essentially the same as the number in an Eulerian reference frame. This makes sense,

because although moving to a stream coordinates reference frame eliminates the horizontal motion of the meanders, it does not eliminate the changes in thermocline slope which are associated with those meanders (e.g. Fig. 10 of Watts et al., 1995). The number of degrees of freedom across the section was determined as follows. First, the integral time scale was determined at each of the HEFR sites (Emery and Thomson, 1997), resulting in an average integral time scale of about 11 days. Next, because the 'time series' of points available in each bin of the stream coordinates section was irregular (ranging from 3–4 points in a single bin on a given day, if the SAF was running parallel to the HEFR line that day, to no observations in a particular bin for weeks), it was necessary to break up the time series for each cross-stream bin into sections one integral time scale in length and then determine how many of the sections contained observations. The resulting number of degrees of freedom ranged from 6 to 20, with the fewest number on the warm side of the SAF and the larger number on the cold side of the SAF (Fig. 11e). Near the SAF core there were about 14 degrees of freedom, which indicates that the measurement errors contribute at most 1–2 cm s^{-1} to the error in the stream coordinates mean. The statistical standard error of the mean ranges from 2 cm s^{-1} at 2000 dbar to 7 cm s^{-1} near the surface for the along-stream velocities and 1 cm s^{-1} at 2000 dbar to 2 cm s^{-1} near the surface for the cross-stream velocities. Therefore, the mean velocities shown in Fig. 11 are accurate to within 1–7 cm s^{-1} over the full water column.

4.2. Example of dynamical implications

The descriptive differences between the stream coordinates mean sections shown in Figs. 11–14 also have an impact on dynamical conclusions which are drawn from the sections. A more complete discussion of the dynamics of the SAF based on the stream coordinates mean section will be presented in a future paper (Meinen et al., submitted for publication), but one example is presented here.

Analytical and numerical models of an inertial jet suggest that the cross-stream gradient of the

along-stream velocity should have a larger magnitude on the cold side of the current (Fofonoff and Hall, 1983; Hall, 1986; Smith et al., 2000). Previous observational estimates of the stream coordinates sections have found conflicting results in this regard. Johns et al. (1995) found that the largest horizontal shear magnitude occurred on the cold side of the Gulf Stream, consistent with the analytical model. Hall (1986) instead found the horizontal shear magnitude to be larger on the warm side of the Gulf Stream at a location fairly close to the later Johns et al. (1995) study. Phillips and Rintoul (2002) found the largest horizontal shear magnitude on the warm side of the SAF. The results from our best section indicate that the largest horizontal shear magnitude is on the cold side of the SAF (Fig. 16), although the asymmetry is weak. In order to explain these disagreements for both the Gulf Stream and for the SAF it is necessary to compare the methods used in developing each of these stream coordinates mean sections. The Hall (1986) Gulf Stream section utilized distances determined under a 'frozen field' assumption and downstream directions determined from the local vertical shear of horizontal velocity. The Phillips and Rintoul (2002) SAF section did the same. The Johns et al. (1995) Gulf Stream section utilized distances from an OI mapped Z_{12} field similar to our use of a mapped Z_6 field in the SAF (the 12°C isotherm is within the main thermocline in the Gulf Stream). For rotating the velocity observations into along-stream and cross-stream components, the Johns et al. (1995) study used a hybrid of the two methods presented earlier; when the local velocity shear exceeded a certain criterion it was used to define the downstream direction, otherwise the mapped Z_{12} field was used.

The Hall (1986) Gulf Stream section and Phillips and Rintoul (2002) SAF section used similar methods, and both observed the stronger magnitude of cross-stream shear of along-stream velocity on the warm side of the respective currents, counter to the analytical model results. The Johns et al. (1995) Gulf Stream section and our SAFDE section used generally similar methods and both studies found that the stronger magnitude of cross-stream shear of along-stream
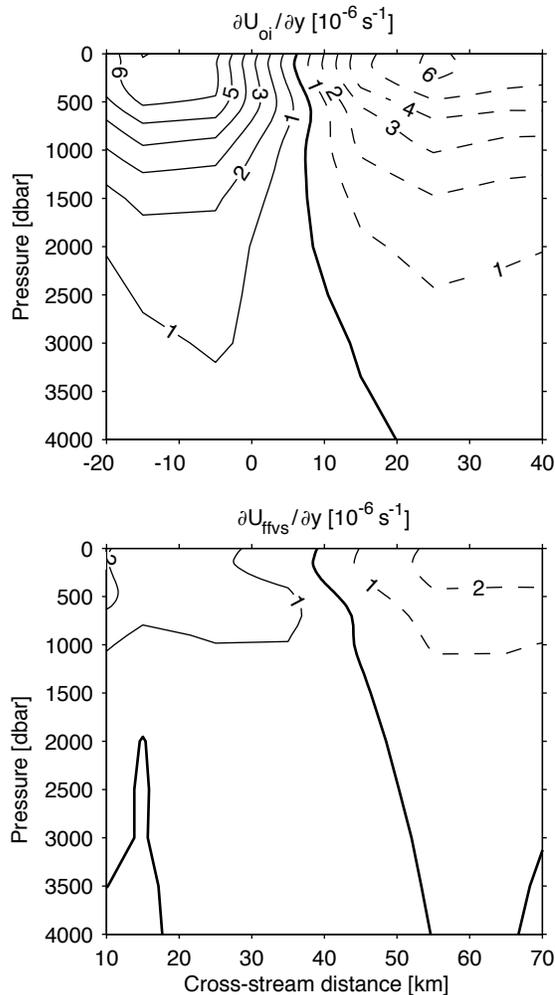
Fig. 16. Cross-stream gradient of the stream coordinates mean along-stream component of the absolute velocity. Dashed contours indicate negative, solid indicates positive. Upper panel shows the gradient of the mean section determined using the OI-mapped distance and direction (Fig. 11), lower panel shows the gradient of the mean section determined using the frozen-field location and vertical shear downstream direction (Fig. 14).

surface, in a study of repeat ADCP sections across the Gulf Stream and they also found the highest shear magnitude on the cold side of the current. While not completely definitive (further studies are required since the Johns et al. (1995) study used a slightly different method than in this study and the Rossby and Zhang (2001) study did not allow for stream curvature), these results suggest that the use of the 'frozen-field' and vertical shear methods provides an erroneous result. Hogg (1992), on the other hand, revisited the Hall (1986) data and suggested that the particular definition of frozen cross-stream distance used by Hall (1986) might have resulted in obtaining the strongest shear magnitude on the 'wrong' side of the Gulf Stream. This ambiguity in frozen field results highlights both the importance of the method used in developing stream coordinates mean sections and also the need for caution in interpreting stream coordinates mean sections previously developed using strong assumptions about the character of the flow and its variability. While studies such as Hall (1986) and Phillips and Rintoul (2002) provided considerable improvements over previous Eulerian mean estimates of the structure of the Gulf Stream and SAF respectively, dynamical interpretation may be better left to stream coordinates sections developed using a more robust method such as those of Johns et al. (1995) and this study.

Acknowledgements

velocity was on the cold side of the front, consistent with the analytical model results. Rossby and Zhang (2001) used a cross-stream distance and downstream direction method similar to the SAFDE study, with the core defined by the location and direction of the velocity maximum rather than an isotherm crossing a pressure

References

Bower, A.S., Hogg, N.G., 1996. Structure of the Gulf Stream and its recirculations at 55° W. Journal of Physical Oceanography 26, 1002–1022.

Bretherton, F.P., Davis, R.E., Fandry, C.B., 1976. A technique for objective analysis and design of oceanographic experiments applied to MODE-73. Deep-Sea Research I 23, 559–582.

Chaplin, G.F., Watts, D.R., 1984. Inverted echo sounder development. IEEE Oceans '84 Conference Record, Vol. 1, pp. 249–253.

Chave, A.D., Luther, D.S., 1990. Low-frequency, motionally induced electromagnetic fields in the ocean: 1. Theory. Journal of Geophysical Research 95, 7185–7200.

Chave, A.D., Luther, D.S., Meinen, C.S. Correction of motional electric field measurements for galvanic distortion. Journal of Atmospheric and Oceanic Technology, submitted for publication.

Emery, W.J., Thomson, R.E., 1997. Data Analysis Methods in Physical Oceanography. Pergamon Press, Oxford.

Fofonoff, N.P., 1962. Dynamics of ocean currents. In: Hill, M.N. (Ed.), The Sea: Ideas and Observations on Progress in the Study of the Seas, 1: Physical Oceanography. Wiley-Interscience, New York, pp. 323–395.

Fofonoff, N.P., Hall, M.M., 1983. Estimates of mass, momentum and kinetic energy fluxes of the Gulf Stream. Journal of Physical Oceanography 13, 1868–1877.

Gille, S.T., 1994. Mean sea surface height of the Antarctic Circumpolar Current from Geosat data: Method and application. Journal of Geophyiscal Research 99, 18255–18273.

Halkin, D., Rossby, H.T., 1985. The structure and transport of the Gulf Stream at 73° W. Journal of Physical Oceanography 15, 1439–1452.

Hall, M.M., 1986. Horizontal and vertical structure of the Gulf Stream velocity field at 68° W. Journal of Physical Oceanography 16, 1814–1828.

Hall, M.M., 1989. Velocity and transport structure of the Kuroshio extension at 35° N, 152° E. Journal of Geophysical Research 94, 14445–14459.

Hogg, N.G., 1992. On the transport of the Gulf Stream between Cape Hatteras and the Grand Banks. Deep-Sea Research I 39, 1231–1246.

Johns, W.E., Shay, T.J., Bane, J.M., Watts, D.R., 1995. Gulf Stream structure, transport, and recirculation near 68° W. Journal of Geophysical Research 100, 817–838.

Kontoyiannis, H., 1997. Quasi-geostrophic modeling of mixed instabilities in the Gulf Stream near 73° W. Dynamics of Atmospheres and Oceans 26, 133–158.

Luther, D.S., Filloux, J.H., Chave, A.D., 1991. Low-frequency, motionally induced electromagnetic fields in the ocean: 2. Electric field and eulerian current comparison. Journal of Geophysical Research 96, 12797–12814.

Luther, D.S., Chave, A.D., Church, J.A., Filloux, J.H., Richman, J.G., Rintoul, S.R., Watts, D.R., 1997. The sub-antarctic flux and dynamics experiment (SAFDE). WOCE Notes 9, 8–12.

Meinen, C.S., 2001. Structure of the North Atlantic Current in stream-coordinates and the circulation in the Newfoundland Basin. Deep-Sea Research I 48, 1553–1580.

Meinen, C.S., Watts, D.R., 2000. Vertical structure and transport on a transect across the North Atlantic Current near 42° N: time series and mean. Journal of Geophysical Research 105, 21869–21891.

Meinen, C.S., Luther, D.S., Watts, D.R., Chave, A.D., Tracey, K.L. Mean stream-coordinates structure of the Subantarctic Front: temperature, salinity, and absolute velocity. Journal of Geophysical Research, submitted for publication.

Meinen, C.S., Luther, D.S., Watts, D.R., Tracey, K.L., Chave, A.D., Richman, J., 2002. Combining Inverted Echo Sounder and Horizontal Electric Field Recorder measurements to obtain absolute velocity profiles. Journal of Atmospheric and Oceanic Technology 19, 1653–1664.

Phillips, H.E., Rintoul, S.R., 2000. Eddy variability and energetics from direct current measurements in the Antarctic Circumpolar Current south of Australia. Journal of Physical Oceanography 30, 3050–3076.

Phillips, H.E., Rintoul, S.R., 2002. A mean synoptic view of the Subantarctic Front south of Australia. Journal of Physical Oceanography 32, 1536–1553.

Rintoul, S.R., Sokolov, S., 2001. Baroclinic transport variability of the Antarctic Circumpolar Current south of Australia (WOCE repeat section SR3). Journal of Geophysical Research 106, 2815–2832.

Rintoul, S.R., Hughes, C., Olbers, D., 2001. The Antarctic Circumpolar Current system. Ocean Circulation and Climate. Academic Press, New York, pp. 271–302 (Chapter 4.6).

Rossby, T., 1987. On the energetics of the Gulf Stream at 73 W. Journal of Marine Research 45, 59–82.

Rossby, T., Zhang, H.-M., 2001. The near-surface velocity and potential vorticity structure of the Gulf Stream. Journal of Marine Research 59, 949–975.

Sanford, T.B., 1971. Motionally-induced electric and magnetic fields in the sea. Journal of Geophysical Research 76, 3476–3492.

Smith, W.H.F., Sandwell, D.T., 1997. Global sea floor topography from satellite altimetry and ship depth soundings. Science 277, 1956–1962.

Smith, R.D., Maltrud, M.E., Bryan, F.O., Hecht, M.W., 2000. Numerical simulation of the North Atlantic Ocean at $\frac{1}{10}^\circ$. Journal of Physical Oceanography 30, 1532–1561.

Watts, D.R., Rossby, H.T., 1977. Measuring dynamic heights with inverted echo sounders: Results from MODE. Journal of Physical Oceanography 7, 345–358.

Watts, D.R., Tracey, K.L., Bane, J.M., Shay, T.J., 1995. Gulf Stream path and thermocline structure near 74° W and 68° W. Journal of Geophysical Research 100, 18291–18312.

Watts, D.R., Sun, C., Rintoul, S., 2001. A two-dimensional gravest Empirical Mode determined from hydrographic observations in the Subantarctic Front. Journal of Physical Oceanography 31, 2186–2209.

Whitworth, III.T., 1983. Monitoring the transport of the Antarctic Circumpolar Current at Drake Passage. Journal of Physical Oceanography 13, 2045–2057.